

## Original Article

**Cite this article:** Yang EL, Kutty S, Soriano BD, Mallenahalli S, Ferguson MR, Lewin MB, and Buddhe S (2021) Is biventricular vascular coupling a better indicator of ventriculo-ventricular interaction in congenital heart disease? *Cardiology in the Young* 31: 2009–2014. doi: [10.1017/S1047951121001426](https://doi.org/10.1017/S1047951121001426)


Received: 8 December 2020  
 Revised: 20 February 2021  
 Accepted: 18 March 2021  
 First published online: 20 April 2021

**Keywords:**

Biventricular interaction; cardiovascular magnetic resonance imaging; congenital heart disease; ventricular–vascular coupling; ventriculo-ventricular intervention

**Address for Correspondence:** Emily Yang, MD, Division of Cardiology, Seattle Children's Hospital, 4800 Sand Point Way NE, Seattle, WA 98105, USA. Tel: (206) 987-2127. E-mail: [emilyyang90@gmail.com](mailto:emilyyang90@gmail.com)

# Is biventricular vascular coupling a better indicator of ventriculo-ventricular interaction in congenital heart disease?

Emily L Yang<sup>1</sup> , Shelby Kutty<sup>2</sup>, Brian D Soriano<sup>1</sup>, Sathish Mallenahalli<sup>1</sup>, Mark R Ferguson<sup>3</sup>, Mark B Lewin<sup>1</sup> and Sujatha Buddhe<sup>1</sup>

<sup>1</sup>Division of Cardiology, Seattle Children's Hospital, Seattle, WA, USA; <sup>2</sup>Division of Cardiology, Taussig Heart Center, Johns Hopkins School of Medicine, Baltimore, MD, USA and <sup>3</sup>Division of Radiology, Seattle Children's Hospital, Seattle, WA, USA

**Abstract**

**Background:** Ventriculo-ventricular interactions are known to exist, though not well quantified. We hypothesised that the ventricular–vascular coupling ratio assessed by cardiovascular MRI would provide insight into this relationship. We also sought to compare MRI-derived ventricular–vascular coupling ratio to echocardiography and patient outcomes. **Methods:** Children with cardiac disease and biventricular physiology were included. Sanz's and Bullet methods were used to calculate ventricular–vascular coupling ratio by MRI and echocardiography, respectively. Subgroup analysis was performed for right and left heart diseases. Univariate and multivariate regressions were performed to determine associations with outcomes. **Results:** A total of 55 patients (age  $14.3 \pm 2.5$  years) were included. Biventricular ventricular–vascular coupling ratio by MRI correlated with each other ( $r = 0.41$ ;  $p = 0.003$ ), with respect to ventricle's ejection fraction ( $r = -0.76$  to  $-0.88$ ;  $p < 0.001$ ) and other ventricle's ejection fraction ( $r = -0.42$  to  $-0.47$ ;  $p < 0.01$ ). However, biventricular ejection fraction had only weak correlation with each other ( $r = 0.31$ ;  $p = 0.02$ ). Echo underestimated ventricular–vascular coupling ratio for the left ventricle ( $p < 0.001$ ) with modest correlation to MRI-derived ventricular–vascular coupling ratio ( $r = 0.43$ ;  $p = 0.002$ ). There seems to be a weak correlation between uncoupled right ventricular–vascular coupling ratio with the need for intervention and performance on exercise testing ( $r = 0.33$ ;  $p = 0.02$ ). **Conclusion:** MRI-derived biventricular ventricular–vascular coupling ratio provides a better estimate of ventriculo-ventricular interaction in children and adolescents with CHD. These associations are stronger than traditional parameters and applicable to right and left heart conditions.

A ventriculo-ventricular interaction is known to exist – as the right and left heart function as two pumps in series with a common blood supply, a common septum, and a shared pericardium. The shared mechanics and haemodynamics of the ventricles create a collective physiology represented in both health and pathology. Thus, the pathology of one ventricle, as in some CHD, results in the pathology of the other initially unaffected ventricle. While observed in many pathologic states, this association is not well quantified as traditional measures of ventricular size and function are limited in their ability to represent the complexity of the cardiac system. To better characterise cardiovascular efficiency and to quantify the relationship between a ventricle and its upstream vasculature, ventricular–vascular coupling ratio was developed. Sunagawa *et al* established the concept of the left ventricle as an elastance in the 1980s by giving the left ventricle and aortic elastance comparable units.<sup>1,2</sup> This is significant as elastance can embody the potential energy of the system. With this framework, ventricular–vascular coupling ratio has since been defined in the following equation (Equation 1):<sup>3–8</sup>

$$VVCR = E_a/E_{es} \quad (1)$$

where VVCR is ventricular–vascular coupling ratio,  $E_a$  is effective arterial elastance, and  $E_{es}$  is end-systolic ventricular elastance.

The effective arterial elastance ( $E_a$ ) is an index of afterload, and the end-systolic ventricular elastance ( $E_{es}$ ) is an index of contractility.<sup>3–8</sup> Initially defined through pressure–volumes loops obtained via right heart catheterisation, the equations for arterial elastance and ventricular elastance were established (Equations 2 and 3).<sup>3</sup>

$$E_{es} = ESP/(ESV - V_0) \quad (2)$$

© The Author(s), 2021. Published by Cambridge University Press. This is an Open Access article, distributed under the terms of the Creative Commons Attribution licence (<http://creativecommons.org/licenses/by/4.0/>), which permits unrestricted re-use, distribution, and reproduction in any medium, provided the original work is properly cited.

$$E_a = ESP/SV \quad (3)$$

where  $E_a$  is effective arterial elastance,  $E_{es}$  is end-systolic ventricular elastance,  $ESP$  is ventricular end-systolic pressure,  $ESV$  is ventricular end-systolic volume, and  $SV$  is arterial stroke volume.

$V_0$  represents a theoretic volume approximated by the volume axis intercept of pressure–volume loops at end-systole. This is to represent the volume of the unloaded ventricle.<sup>1,2</sup> Though not well studied,  $V_0$  is often assumed to be negligible in calculations of ventricular elastance.<sup>3</sup> With these definitions and assumptions, ventricular–vascular coupling ratio simplifies down further (Equation 4).<sup>3</sup>

$$VVCR = ESV/SV \quad (4)$$

where  $VVCR$  is ventricular–vascular coupling ratio,  $ESV$  is ventricular end-systolic volume, and  $SV$  is arterial stroke volume.

This represents an efficient ventricular–vascular interaction where the needed arterial stroke volume is transferred to the periphery with the least possible energy expenditure. In contrast, an uncoupled system, represented by ventricular–vascular coupling ratio  $>1$ , signifies inefficient or failing cardiac function.<sup>3,6,7,9</sup>

Initially collected by catheterisation, through pressure–volume loops with varying IVC occlusion to adjust preload, these concepts have since been applied to non-invasive modalities including magnetic resonance and echocardiographic imaging. Though right heart catheterisation remains the gold standard, there is an increasing push towards non-invasive measures, particularly within paediatrics.<sup>3–7</sup>

Prior research has focused on ventricular–vascular coupling ratio and its applications to isolated right- or left-sided pathology. In such cases, the measured ventricular–vascular coupling ratio is considered in isolation from the other ventricular–arterial system. Our primary aim was to look at similar patients via non-invasive imaging to evaluate a hypothesised ventriculo-ventricular interaction. We suspected that the uncoupling of a respective ventricular–arterial system with left- or right-sided disease causes a similar uncoupling in the paralleled circuit. Our secondary aim was the compare ventricular–vascular coupling ratio calculations by the non-invasive measures of cardiovascular MRI and echocardiography.

## Materials and methods

Patients were enrolled retrospectively from a database of cardiac MRI studies obtained between January, 2008 and December, 2018 at the Seattle Children’s Hospital. Patients who underwent cardiac MRI and echocardiogram within 6 months of each other were considered. Other inclusion criteria included biventricular physiology and either known as right- or left-sided congenital cardiac lesions. In addition, for the purpose of assessing clinical outcomes, patients also had to have obtained cardiopulmonary exercise testing as per clinical indication within 5 years of their cardiac MRI. Cardiopulmonary exercise testing was largely performed on bike ergometer as per institutional protocols. A few exceptions underwent testing by treadmill due to the inability to comprehend biking instructions. Patients with interval intervention, surgical, or catheter-based between cardiac MRI and cardiopulmonary exercise testing were excluded.

Traditional measures of biventricular size and systolic function were assessed by both MRI and echocardiography. Ventricular–vascular coupling ratio for both modalities was also determined

as described below. Study was approved by the Institutional Review Board at the Seattle Children’s Hospital.

## Ventricular–vascular coupling ratio by cardiovascular magnetic resonance

Cardiac MRIs were performed on a Siemens 1.5 T Magnetom Avanto platform (Siemens Medical Solutions USA, Erlangen, Germany) per institutional protocol. The analysis was performed either on a CMR42 (Circle Cardiovascular Imaging Inc., Calgary, Alberta, Canada) or a Leonardo workstation using Siemens analytic software (Argus, Siemens Medical Solutions, Erlangen, Germany). Traditional measurements were obtained and analyzed via standard techniques. Ventricular–vascular coupling ratio was determined using Sanz’s approach and the equation is outlined below (Equation 4).<sup>3,6,7</sup>

$$VVCR = ESV/SV \quad (4)$$

where  $VVCR$  is ventricular–vascular coupling ratio,  $ESV$  is ventricular end-systolic volume, and  $SV$  is arterial stroke volume.

The ventricular end-systolic volume is calculated by tracing the ventricular endocardial silhouette in end-systole. Similar tracings are performed at end-diastole for ejection fraction calculations. In a similar manner, the inner contours of the main vessels were traced to determine area and flow rates from which stroke volume was determined.

## Ventricular–vascular coupling ratio by echocardiogram

All transthoracic echocardiograms were performed using an iE33 ultrasound system (Philips Medical System, Andover, MA, USA). Standard images were obtained as per institutional protocol and stored in digital format for offline analysis using Syngo Dynamics workstation (Siemens Medical Solutions USA, Syngo Dynamic Solutions, Ann Arbor, MI, USA). Traditional echocardiographic parameters of left ventricle systolic function were analysed using standard techniques in accordance with the American Society of Echocardiography guidelines. The end-systolic volume, end-diastolic volume, stroke volume, and ejection fraction were measured using the Bullet method (Equations 5, 6, and 7).<sup>8</sup> These were then applied to Equation 4 to determine ventricular–vascular coupling ratio by echocardiogram.

$$ESV = 5/6 LVA_S \times L_S \quad (5)$$

$$EDV = 5/6 LVA_D \times L_D \quad (6)$$

$$SV = EDV - ESV \quad (7)$$

where  $ESV$  is ventricular end-systolic volume,  $LVA_S$  is left ventricular area at end-systole,  $L_S$  is left ventricular length at end-systole,  $EDV$  is ventricular end-diastolic volume,  $LVA_D$  is left ventricular area at end-diastole,  $L_D$  is left ventricular length at end-diastole, and  $SV$  is arterial stroke volume.

The left ventricular area was measured as an orthogonal cross-section in a parasternal short window at the mid-papillary muscle in both end-systole and end-diastole ( $LVA_S$  and  $LVA_D$ ). Length is measured from the mitral annulus to the apex in an apical four-chamber view, again in both end-systole and end-diastole ( $L_S$  and  $L_D$ ). These are multiplied by a constant variable of 5/6 determined through modelling the left ventricle as a bullet-shaped structure.

**Table 1.** Patient demographics and diagnoses (n = 55)

Age (years)	14.3 ± 2.5
Male gender	31 (56%)
Weight (kg)	58 ± 19
BSA (m <sup>2</sup> )	1.6 ± 0.3
Right heart disease	44 (80%)
Left heart disease	11
Primary cardiac diagnosis	
Tetralogy of Fallot	41 (75%)
Aortic valve stenosis	5
Left ventricular outlet obstruction	3
Pulmonary valve stenosis	2
Dilated cardiomyopathy	1
Left ventricular hypertrophy	1
Right ventricular outlet obstruction	1
Transposition of the great arteries	1

Data are expressed as mean ± standard deviation; number (percentage).  
BSA = body surface area.

### Statistical analysis

Patient data were compiled and reported as mean and standard deviation, or as median values and ranges for continuous variables. Subgroup analysis was performed for right and left heart diseases. Univariate and multivariate regressions were performed to determine associations with outcomes. In addition, Pearson's correlation coefficients were calculated to determine the strength of relationships. All statistical analyses were performed using SPSS 19.0 (SPSS Inc., Chicago, IL, USA). Statistical significance was defined as  $p < 0.05$ .

### Results

A total of 55 patients met the inclusion criteria for this study. All patients had biventricular physiology, 11 with primary left heart disease and 44 with primary right heart disease. Primary cardiac diagnoses are further broken down in Table 1. Patients were aged 8–27 at the time of cardiac MRI with a mean age of  $14.3 \pm 2.5$  years. Their mean weight was  $58 \pm 19$  kg and mean body surface area  $1.6 \pm 0.3$  m<sup>2</sup> (Table 1).

Ventricular–vascular coupling ratio calculations, as well as traditional measures of ventricular function, were evaluated by cardiac MRI. These results are represented in Table 2. The mean MRI-derived ventricular–vascular coupling ratio for the left ventricle was  $0.83 \pm 0.29$  ( $0.72 \pm 0.34$  for left heart disease and  $0.84 \pm 0.29$  for right heart disease) and for the right ventricle was  $1.71 \pm 0.93$  ( $0.95 \pm 0.43$  for left heart disease and  $1.89 \pm 0.93$  for right heart disease). In comparison, the mean echo-derived ventricular–vascular coupling ratio of the left ventricle was  $0.65 \pm 0.15$  ( $p < 0.001$ ) and it was  $0.59 \pm 0.12$  for left heart disease and  $0.66 \pm 0.16$  for right heart disease. This moderately correlates to the MRI-derived ventricular–vascular coupling ratio of the left ventricle ( $r = 0.43$ ;  $p = 0.002$ ), though consistently underestimating it (Fig 1). Other traditional measures of ventricular function included MRI-derived left ventricular ejection fraction  $57\% \pm 11\%$  and MRI-derived right ventricular ejection fraction  $50\% \pm 10\%$ .

**Table 2.** Collective CMR and ECHO-derived data

CMR LV VVCR	$0.83 \pm 0.29$
CMR Ao SV (ml)	$69 \pm 24$
CMR LV ESV (ml)	$57 \pm 20$
CMR RV VVCR	$1.71 \pm 0.93$
CMR MPA SV (ml)	$76 \pm 26$
CMR RV ESV (ml)	$114 \pm 45$
CMR LV EF%	$57 \pm 11$
CMR RV EF%	$50 \pm 10$
CMR LV mass (g)	$103 \pm 52$
CMR Ao RF%	1 (0–77)
CMR MPA RF%	34 (0–59)
ECHO LV VVCR	$0.65 \pm 0.15$
ECHO LV SV (ml)	$95 \pm 34$
ECHO LV ESV (ml)	$60 \pm 21$
Peak VO <sub>2</sub> (ml/kg/min)	$31 \pm 8$

Data are expressed as mean ± standard deviation; median (range).

Ao: aorta = CMR = cardiac magnetic resonance imaging; EF = ejection fraction; ESV = end-systolic volume; LV = left ventricle; MPA = main pulmonary artery; RF = regurgitant fraction; RV = right ventricle; SV = stroke volume; VO<sub>2</sub> = oxygen consumption; VVCR = ventricular–vascular coupling ratio.

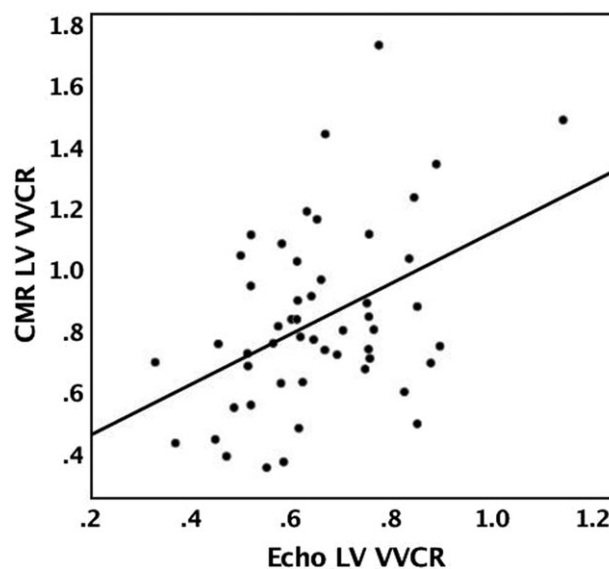


**Figure 1.** Correlation between MRI and ECHO-derived ventricular–vascular coupling ratio of the left ventricle. CMR: cardiac magnetic resonance imaging; LV: left ventricle; VVCR: ventricular–vascular coupling ratio.

Comparison of MRI-derived ventricular–vascular coupling ratio for the right and left ventricles reveals a modest correlation ( $r = 0.41$ ;  $p = 0.003$ ) (Fig 2). In addition, we found a modest correlation between MRI-derived ventricular–vascular coupling ratio with its respective ejection fraction ( $r = -0.76$  to  $-0.88$ ;  $p < 0.001$ ) (Fig 3), as well as the ejection fraction of the other ventricle ( $r = -0.42$  to  $-0.47$ ;  $p < 0.01$ ). However, biventricular ejection fraction had only weak correlation with each other ( $r = 0.31$ ;  $p = 0.02$ ) (Fig 4).

Thirty patients (54%) of the right heart disease patients required interventions at median of 12.7 months (range 0.6–61.0 months) following MRI. Surgical interventions were required in 21 patients when compared to 9 catheter-based interventions

**Table 3.** Interventions in study patients

Patients needing pre-CMR repair	51
Patients needing post-CMR intervention	30
Type of post-CMR intervention	
Surgical	21 (70%)
Catheter-based	9

Data are expressed as raw numbers (percentage).  
CMR = cardiac magnetic resonance imaging.

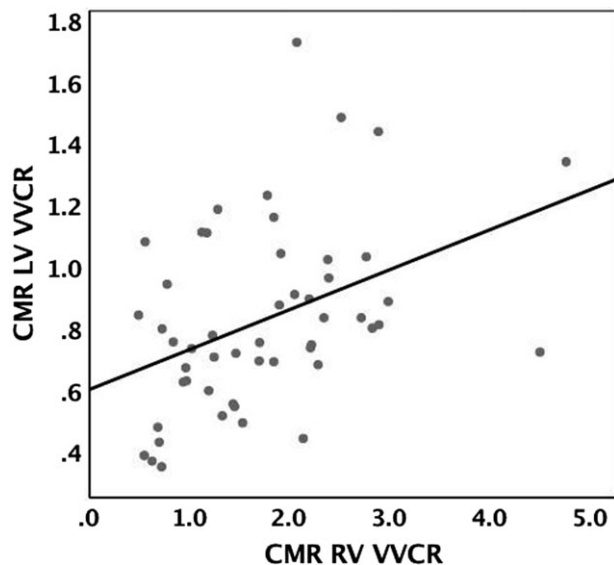


**Figure 2.** Evidence of biventricular interaction by ventricular-vascular coupling ratio, correlation between the ventricular-vascular coupling ratio of the left ventricle and right ventricle. CMR: cardiac magnetic resonance imaging; LV: left ventricle; RV: right ventricle; VVCR: ventricular-vascular coupling ratio.

(Table 3). A majority of these were valve replacements (22 of the 30, or 73%). Mean MRI-derived ventricular-vascular coupling ratio for the right ventricle was significantly higher in the group with interventions ( $1.9 \pm 1.0$ ) compared to others ( $1.4 \pm 0.7$ ;  $p < 0.05$ ), while traditional functional parameters were not significantly different (Fig 5).

All patients included in the study underwent cardiopulmonary exercise testing, though 5 studies (9%) were deemed submaximal. Most studies (53 of 55, or 96%) were performed on bike ergometer. Mean MRI-derived ventricular-vascular coupling ratio for the right ventricle also had some weak correlation to peak maximal oxygen consumption as obtained from cardiopulmonary exercise testing ( $r = 0.33$ ;  $p = 0.02$ ) (Fig 6), while traditional measures of ventricular function had no significant association.

When subgroup analysis was performed separately for left and right heart disease, the association with ventricular-vascular coupling ratio between the other ventricle's ventricular-vascular coupling ratio stayed significant with ( $r = 0.85$ ;  $p = 0.02$ ) for left heart disease and ( $r = 0.40$ ;  $p = 0.008$ ) for right heart disease, unlike traditional ejection fraction measurements.

## Discussion

A ventriculo-ventricular interaction is known to exist, though it may not be well quantified by traditional measures of ventricular

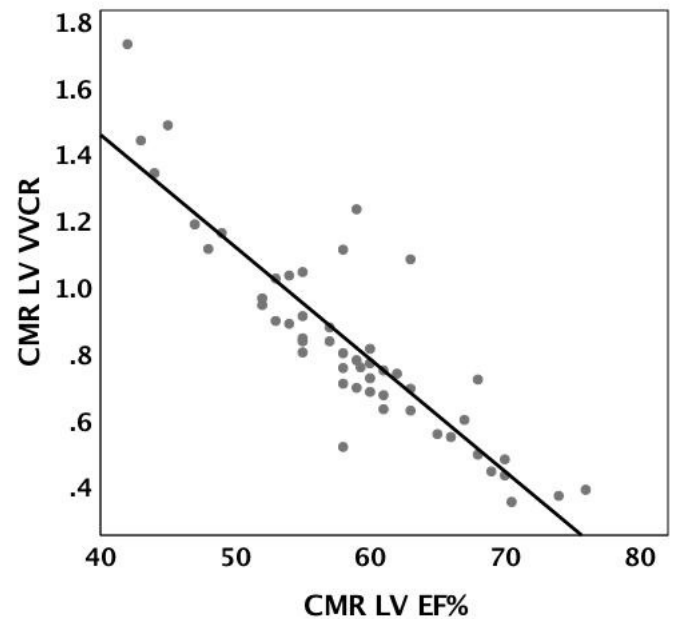


**Figure 3.** Correlation between MRI-derived ventricular-vascular coupling ratio of the left ventricle and left ventricular ejection fraction. CMR: cardiac magnetic resonance imaging; EF: ejection fraction; LV: left ventricle; VVCR: ventricular-vascular coupling ratio.

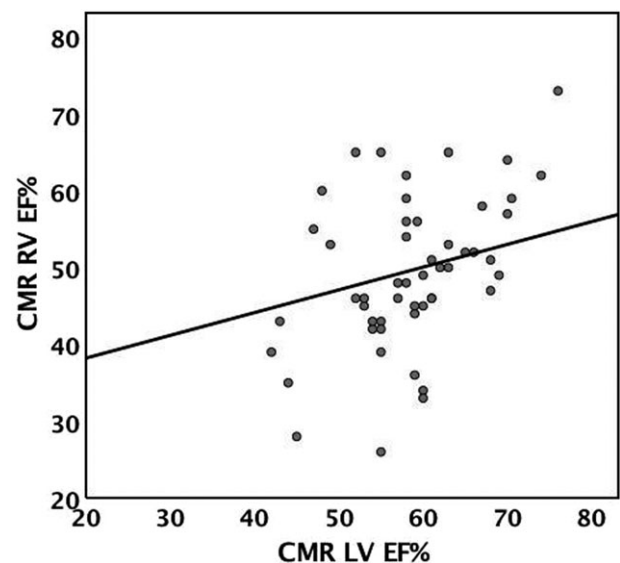


**Figure 4.** Correlation between the MRI-derived ejection fraction of the left ventricle and right ventricle. CMR: cardiac magnetic resonance imaging; EF: ejection fraction; LV: left ventricle; RV: right ventricle.

function.<sup>10–15</sup> Clyne et al published a review in the 1980s to demonstrate this interdependence by describing its structural, haemodynamic, and functional components.<sup>13</sup> With such complex and multifaceted physiology, it is reasonable to expect that a more comprehensive surrogate for the systolic function is needed to appreciate this relationship between the right and left ventricles. For example, ventricular-vascular coupling ratio which reflects the ventriculo-arterial relationship, as demonstrated in this study,



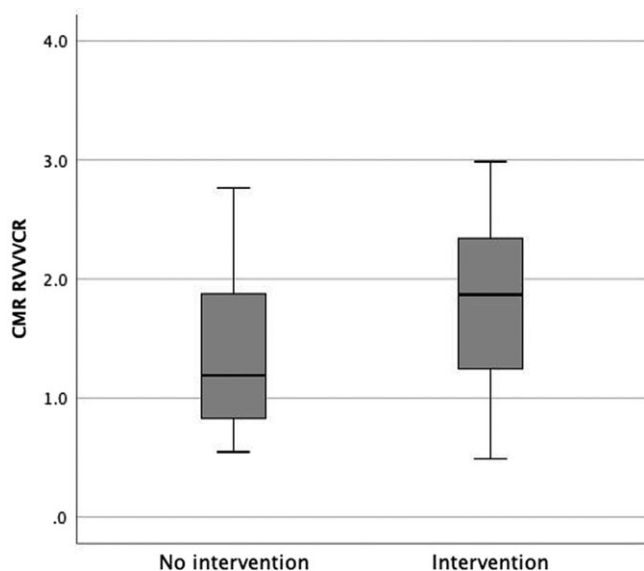


**Figure 5.** Need for intervention and MRI-derived ventricular-vascular coupling ratio of the right ventricle. CMR: cardiac magnetic resonance imaging; RVVWCR: ventricular-vascular coupling ratio of the right ventricle.

appears to better estimate the biventricular relationship.<sup>3,6,7,9</sup> When compared to ejection fraction, which does not adequately reflect biventricular uncoupling, ventricular-vascular coupling ratio incorporates ventriculo-arterial stiffening or compliance into its calculations.<sup>4,5,14</sup> As such, some component of the contralateral uncoupling in the isolated right- or left-sided disease likely relates to the increasing upstream arterial stiffness ( $E_a$ ) or decreasing ventricular compliance ( $E_{es}$ ). For right-sided disease, increasing end-systolic volumes would impede left-sided function with leftward bowing of their shared septum. This septal displacement, as well as mechanical discoordination between the septum and right ventricle free wall results in decreased contractility of the left ventricle.<sup>13,16</sup> Changes in septal geometry also cause altered left ventricle torsion resulting in decreased left ventricle efficacy. Decreased left ventricle torsion rate also results in decreased mechanical energy transfer from the left ventricle to right ventricle, resulting in subsequent declines in right ventricle function.<sup>17</sup> In the setting of right ventricular pressure overload, a hypertrophy of the right ventricle can result in diminished right ventricle compliance and decreased output, which can be seen downstream as decreased left ventricle output over time.<sup>13</sup> Similar effects could also be seen with left-sided lesions. In addition, considering the right and left heart as two haemodynamic systems in series, increasing arterial stiffness and afterload in aortic valve pathology could chronically result in increased pressures downstream leading to a similar biventricular uncoupling. Many factors likely contribute to the biventricular uncoupling seen in CHD.<sup>10,13,14,17</sup> Further analysis of arterial and ventricular contributions to the uncoupling ventricular-vascular coupling ratio would likely provide further insight into this relationship. Also, while the biventricular interaction remained significant on multivariate analysis for right and left-sided disease, more patients with left-sided pathology would allow for additional investigations into each ventricle's contribution to the interdependence. And such an understanding would allow for further characterisation and justification of the biventricular uncoupling. Even though the ventricular-vascular coupling ratio of the left ventricle correlates nicely to the left ventricular

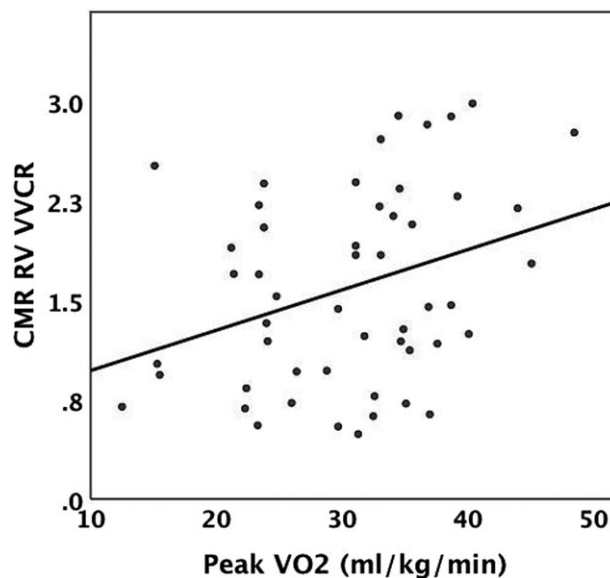


**Figure 6.** Correlation between MRI-derived ventricular-vascular coupling ratio and peak VO<sub>2</sub>. CMR: cardiac magnetic resonance imaging; RV: right ventricle; VO<sub>2</sub>: oxygen consumption; VVCR: ventricular-vascular coupling ratio.

ejection fraction, as they are mathematically related, it is interesting to note that the population represented in this study appears healthy from an ejection fraction standpoint, but not by ventricular-vascular coupling ratio. This again suggests that ventricular-vascular coupling ratio provides more critical information than ejection fraction, which fails to account for downstream effects of arterial compliance of the ventricular function.

As a secondary goal, this study compared ventricular-vascular coupling ratio calculations by cardiac MRI and echocardiography. While a clear correlation exists between MRI-derived and echo-derived ventricular-vascular coupling ratio, it was found that echocardiography consistently underestimated the coupling. This discrepancy may be explained by echocardiography underpredicting end-systolic volume, overpredicting stroke volume, or a combination of both when compared to cardiac MRI. Prior studies assessing the Bullet method of echocardiography have found that it underestimates volumes when compared to cardiac MRI.<sup>18–20</sup> As such, a discrepancy in end-systolic volume most likely explains our findings. The assumptions of Bullet method include that the left ventricle is bullet shaped and as such the left ventricular volume maybe be approximated by measurements taken in a single frame multiplied by a fixed correction factor, 5/6 or 0.83.<sup>18–22</sup> The error likely occurs secondary to these assumptions. In addition, some variation may be attributed to the averaging over multiple heartbeats for cardiac MRI calculations when compared to echo data that is collected over a single heartbeat. Further comparison to calculations by right heart catheterisation would be beneficial to further assess both non-invasive measures.

Lastly, this study revealed a correlation between worse MRI-derived ventricular-vascular coupling ratio for the right ventricle and the need for intervention. While not significant in left-sided pathology, we suspect the small sample size of left-sided cardiac lesions contributed to the finding. The findings for the right ventricle suggest a clinical application of trending ventricular-vascular coupling ratio to help guide the need for and timing of interventions. Further longitudinal studies are needed to better explore this finding. The correlation, albeit a weak correlation, between MRI-

derived ventricular–vascular coupling ratio for the right ventricle and maximal oxygen consumption further emphasises the clinical significance of ventricular–vascular coupling ratio, and in that, it relates to exercise intolerance. No additional conclusions may be drawn from the data collected by cardiopulmonary exercise testing. We suspect these findings were limited by the number of submaximal studies (9%), as well as the inherent limitations of performing cardiopulmonary exercise testing in the paediatric population with variability in performance and compliance.

### Study limitations

This study was conducted retrospectively. The study was also limited by small sample size, particularly with regards to left-sided cardiac disease. Images were collected in the paediatric population, occasionally resulting in limited echocardiogram windows. The study population is heterogeneous with regards to cardiac pathology, particularly in that both right and left-sided diseases were included, though many of the patients had right heart disease. While the association with the ventricular–vascular coupling ratio and the other ventricle's ventricular–vascular coupling ratio remained significant on subgroup analysis for left and right heart diseases, the heterogeneity of our combined population likely affected results. Specifically, we wonder whether stronger correlations exist within a single disease state.

### Conclusions

MRI-derived biventricular ventricular–vascular coupling ratio appears to provide an estimate of the ventriculo-ventricular interaction in children and adolescents with CHD, which has otherwise not been well quantified. These associations are stronger than traditional parameters and applicable to right and left heart conditions. Echo-derived ventricular–vascular coupling ratio for the left ventricle consistently underestimated the coupling. Worse MRI-derived ventricular–vascular coupling ratio for the right ventricle in patients requiring interventions suggests its potential clinical value, which should be further investigated in longitudinal studies.

**Acknowledgements.** None.

**Financial Support.** This research received no specific grant from any funding agency, commercial, or not-for-profit sectors.

**Conflicts of interest.** None.

**Ethical standards.** The authors assert that all procedures contributing to this work comply with the ethical standards of the relevant national guidelines on human experimentation (National Commission for the Protection of Human Subjects of Biomedical and Behavioral Research) and with the Helsinki Declaration of 1975, as revised in 2008, and has been approved by the Institutional Review Board at Seattle Children's Hospital.

### References

1. Sunagawa K, Maughan WL, Sagawa K. Optimal arterial resistance for the maximal stroke work studied in isolated canine left ventricle. *Circ Res* 1985; 56: 586–595.
2. Sasayama S, Asanoi H. Coupling between the heart and arterial system in heart failure. *Am J Med* 1991; 90: 14S–18S.
3. Sanz J, García-Alvarez A, Fernández-Friera L, et al. Right ventriculo-arterial coupling in pulmonary hypertension: a magnetic resonance study. *Heart* 2012; 98: 238–243.
4. Saiki H, Eidem BW, Ohtani T, Grogan MA, Redfield MM. Ventricular-arterial function and coupling in the adult Fontan circulation. *J Am Heart Assoc* 2016; 5: e003887.
5. Loeper F, Oosterhof J, van den Dorpel M, et al. Ventricular-vascular coupling in Marfan and non-Marfan Aortopathies. *J Am Heart Assoc* 2016; 5: e003705.
6. Latus H, Binder W, Kerst G, Hofbeck M, Sieverding L, Apitz C. Right ventricular-pulmonary arterial coupling in patients after repair of tetralogy of Fallot. *J Thorac Cardiovasc Surg* 2018; 146: 1366–1372.
7. Truong U, Patel S, Kheyfets V, et al. Non-invasive determination by cardiovascular magnetic resonance of right ventricular-vascular coupling in children and adolescents with pulmonary hypertension. *J Cardiovasc Magn Reson* 2015; 17: 81.
8. Antonini-Canterin F, Poli S, Vriz O, Pavan D, Bello V Di, Nicolosi GL. The ventricular-arterial coupling: from basic pathophysiology to clinical application in the echocardiography laboratory. *J Cardiovasc Echogr* 2013; 23: 91–95.
9. Kubba S, Davila CD, Forfia PR. Methods for evaluating right ventricular function and ventricular-arterial coupling. *Prog Cardiovasc Dis* 2016; 59: 42–51.
10. Li K, Santamore W. Contribution of each wall to biventricular function. *Cardiovasc Res* 1993; 27: 192–800.
11. Lin ACW, Seale H, Hamilton-Craig CJ. Quantification of biventricular strain and assessment of ventriculo-ventricular interaction in pulmonary arterial hypertension using exercise cardiac magnetic resonance imaging and myocardial feature tracking. *J Magn Reson Imaging* 2018; 49: 1427–1436.
12. Penny D, Redington A. Function of the left and right ventricles and the interactions between them. *Pediatr Crit Care Med* 2016; 17: S112–118.
13. Clyne C, Alpert J, Benotti J. Interdependence of the left and right ventricles in health and disease. *Am Hear J* 1989; 117: 1366–1373.
14. Santamore WP, Dell'Italia LJ. Ventricular interdependence: significant left ventricular contributions to right ventricular systolic function. *Prog Cardiovasc Dis* 1998; 40: 289–308.
15. Naeije R, Badagliacca R. The overloaded right heart and ventricular interdependence. *Cardiovasc Res* 2017; 113: 1474–1485.
16. Driessen MMP, Hui W, Bijnens BH, et al. Adverse ventricular-ventricular interactions in right ventricular pressure load: Insights from pediatric pulmonary hypertension versus pulmonary stenosis. *Physiol Rep* 2016; 4: e12833.
17. Dufva MJ, Truong U, Tiwari P, Ivy DD, Shandas R, Kheyfets VO. Left ventricular torsion rate and the relation to right ventricular function in pediatric pulmonary arterial hypertension. *Pulm Circ* 2018; 8: 1–10.
18. Madueme PC, Mazur W, Hor KN, Germann JT, Jefferies JL, Taylor MD. Comparison of area-length method by echocardiography versus full-volume quantification by cardiac magnetic resonance imaging for the assessment of left atrial volumes in children, adolescents, and young adults. *Pediatr Cardiol* 2014; 35: 645–651.
19. Tretter JT, Chakravarti S, Bhatla P. Use of echocardiographic subxiphoid five-sixth area length (bullet) method in evaluation of adequacy of borderline left ventricle in hypoplastic left heart complex. *Ann Pediatr Cardiol* 2015; 8: 243–245.
20. Grosse-Wortmann L, Yun T, Al-Radi O, Kim S, Nii M, Lee K. Borderline hypoplasia of the left ventricle in neonates: Insights for decision-making from functional assessment with magnetic resonance imaging. *J Thorac Cardiovasc Surg* 2008; 136: 1429–1436.
21. Nielsen JC, Lytrivi ID, Ko HH, et al. The accuracy of echocardiographic assessment of left ventricular size in children by the 5/6 area x length (bullet) method. *Echocardiography* 2010; 27: 691–695.
22. Lu JC, Ensing GJ, Yu S, Thorsson T, Donohue JE, Dorfman AL. 5/6 Area length method for left-ventricular ejection-fraction measurement in adults with repaired tetralogy of Fallot: comparison with cardiovascular magnetic resonance. *Pediatr Cardiol* 2013; 34: 231–239.